Electron impact electronic excitation of benzene: Theory and experiment

Alan Falkowski, Romarly da Costa, Marco Lima, Alexi de A. Cadena, Ronald Pocoroba, Regan Jones, Mahak Mathur, J. Childers, Murtadha Khakoo, Fábris Kossoski

Electron impact electronic excitation of benzene: theory and experiment

Alan G. Falkowski,[1] Romarly F. da Costa,[2] Marco A. P. Lima,[3] Alexi de A. Cadena,[4] Ronald Pocoroba,[4] Regan Jones,[4] Mahak Mathur,[5] J. G. Childers,[4] Murtadha A. Khakoo,[4] and Fábris Kossoski[6]

[1)]*Instituto de Física "Gleb Wataghin", Universidade Estadual de Campinas, Campinas, Brazil*

[2)]*Centro de Ciências Naturais e Humanas, Universidade Federal do ABC, 09210-580 Santo André, São Paulo, Brazil*

[3)]*Instituto de Física "Gleb Wataghin", Universidade Estadual de Campinas, Campinas, Brazil*

[4)]*Physics Department, California State University, Fullerton CA 92831, USA*

[5)]*Troy High School, 2200 Dorothy Lane, Fullerton, CA 92831, USA*

[6)]*Laboratoire de Chimie et Physique Quantiques (UMR 5626), Université de Toulouse, CNRS, UPS, 31062 Toulouse, France*

(*Electronic mail: fkossoski@irsamc.ups-tlse.fr)

(*Electronic mail: mkhakoo@fullerton.edu)

(Dated: 5 October 2023)

We report experimental differential cross sections (DCSs) for electron impact excitation of bands I to V of benzene, at incident energies of 10, 12.5, 15, and 20 eV. They are compared to calculations using the Schwinger multichannel method while accounting for up to 437 open channels. For intermediate scattering angles, the calculations reveal that the most intense band (V) emerges from surprisingly similar contributions from all its the underlying states (despite some preference for the dipole-allowed transitions). They further shed light on the intricate multichannel couplings between the states of bands I to V and the higher-lying Rydberg states. In turn, the measurements support a vibronic coupling mechanism for excitation of bands II and IV, and also show an unexpected forward peak in the spin-forbidden transition accounting for band III. Overall, there is decent agreement between theory and experiment at intermediate angles and at lower energies, and in terms of the relative DCSs of the five bands. Discrepancies between the present and the previous experiment regarding bands IV and V draw attention to the need of additional experimental investigations. We also report measured DCSs for vibrational excitation of the combined C−H stretching modes.

I. INTRODUCTION

Benzene is an excellent target molecule for investigations at a fundamental level,[1] given its high symmetry and unique physical-chemical properties, being the prototypical aromatic compound. Benzene and its derivatives can be found in interstellar medium,[2] detergents,[3] plastic production[4] and their usage risks (for example, due to its carcinogenicity),[5,6] combustion environments (as a component of gasoline),[7,8] plasma catalysis,[9] explosives,[10] among others. Free electrons can play an important role in driving the chemistry of several of these environments, by exciting internal degrees of freedom of their constituent species. In view of these fundamental and applied motivations, electronic excitation of benzene via electron collisions has been the subject of numerous studies.[11–27] Based on the these electron energy loss studies, but also photoabsorption[28–30] and multiphoton ionization[31,32] spectroscopy results, and supported by theoretical calculations[33–35] the five electronic bands of benzene (below ≈ 7.5 eV) are fairly well characterized and understood.

However, despite the considerable attention that electron collisions with benzene has received (see Ref.[36] and references therein), there is a single report so far on measured differential cross sections (DCSs) for electronic excitation,[27] to the best of our knowledge. In that contribution, Kato *et al.*[27] presented DCSs as well as integral cross sections (ICSs) for excitation of bands IV and V of benzene, for three impact energies. There is still no available DCSs for the lower-lying bands though. Furthermore, the limited data for benzene contrasts with the recent measurements of DCSs for electronic excitation of related aromatic systems, including pyrimidine,[37] phenol,[38] and *para*-benzoquinone.[39] Finally, García-Abenza *et al.* have very recently proposed a dataset of cross sections for benzene, while drawing attention to the need for more complete and accurate individual cross section, in particular for electronic excitation.[40]

From the theoretical side, describing the electronic excitation of molecules by the impact of electrons is a formidable challenge.[37,41–45] Of relevance to the present study, we notice that any molecular system has an infinite number of Rydberg states below their corresponding ionization potentials. The natural question is how to handle the infinite Rydberg series in the calculations in order to obtain reasonably converged observables,[46] in particular electronic excitation cross sections.

In light of the above motivations, here we report measured and calculated DCSs for electronic excitation of the five lower-lying bands of benzene. The present contribution thus complements our recent experimental-theoretical collaboration on elastic electron scattering from benzene.[46] We provide the first set of DCSs for the three lower-lying bands, and also present new results for bands IV and V, comparing them with the only available result, from Kato *et al.*[27] Experimental DCSs for the vibrational excitation associated with the C−H stretching modes are also reported.

The electron scattering calculations were performed with the Schwinger multichannel method (SMC)[47–49] implemented

with pseudopotentials,[50] while exploring how particular methodological choices affect the computed electronic excitation DCSs. We address the role of including higher-lying Rydberg states in the calculations and of treating states just above the ionization threshold as closed or open channels. In this sense, the present report also expands on a preliminary study on the same questions.[36] The goal of this comprehensive set of calculations is to shed some light on which aspects of the theoretical models deserve further development.

In Section II we describe the experimental techniques, while Section III summarizes the theoretical methods employed in the present study. Section IV contains the results and discussion, and finally, in Section V, we outline our conclusions and future perspectives.

II. EXPERIMENTAL METHOD

The experimental setup has been detailed in Cadena *et al.*[46] which deals with elastic electron scattering. Here, inelastic scattering of benzene is involved and the experimental method follows that given in the inelastic CO papers of Zawadzki *et al.*[51,52] Briefly, the spectrometer was employed with an overall energy resolution of ≈ 80 meV, full-width at half-maximum (FWHM), and an incident electron beam with currents of 30 to 50 nA. The angular resolution of the analyzer was 2.5° FWHM. Molybdenum collimating apertures were installed in both parts to define the incident electron beam and the scattered electron angle (θ), which ranged from θ of 10° to 130°. The electron beam from the monochromator intersected a collimated gas beam of benzene formed by the effusive flow of the gas through a 0.025 mm thick, ≈ 0.4 mm diameter aperture located ≈ 6 mm below the electron beam axis at the center of a crossed beam geometry collision region. Electrons were detected by a discrete dynode electron multiplier with a dark count-rate of < 0.01 Hz.[53] The entire experiment (pumped by a clean pumping $10''$ diameter Diffstak^{TM} diffusion pump equipped with a cold Freon baffle of ≈ -80°C) was housed in a stainless steel, high vacuum chamber that with a base pressure of $\approx 1\times10^{-7}$ Torr, and which rose to $\approx 1.5\times10^{-6}$ Torr when benzene vapor was admitted into the system. The vacuum tank was lined with a dual layer mu-metal shield, which reduced the penetration of terrestrial magnetic fields into the experiment to ≈ 2 mG. The incident electron energy (E_0) ranged from 10 eV to 20 eV and the E_0 scale of the beam was determined with He and calibrated against the well-known He elastic scattering resonance at 19.366 eV.[54] The analyzer was mounted onto a precise lazy susan turntable in such a way that it could be located at θ using a computer-controlled stepper motor setup. The gun and analyzer were both heated by magnetic-field free biaxial resistive heaters[55] to minimize surface contaminants and the clean diffusion pump system ensured (generally) a long term stability of the electron beam (> 6 months continuous operation) with non-corrosive standard gases. However, benzene impacted by electrons seemed to produce reactive radicals that rapidly deposited insulating compounds around and in the spectrometer apertures. Consequently raising the operating pressure above $\approx 2\times10^{-6}$ Torr lowered the electron beam duty time to about 10 days and meant regular cleaning of the gun while we ran the experiment, every 2 to 3 weeks. At the energies surveyed here, many different species could be generated by electron impact excitation[56–59] and singly and doubly ionization[60–64] of benzene. At lower energies, dissociative electron attachment can also occur. In gas-phase conditions, $C_6H_5^-$, $C_2H_2^-$ and their corresponding radical counterparts are produced,[65] whereas in a cluster environment, linear $C_6H_6^-$ has recently been observed.[66] The collimated gas source was mounted on a moveable source arrangement as described in Ref. 67, where the scattered electron background could be expediently and accurately determined by moving the gas source in and out of the collision region. Electronic excitation ICSs and momentum transfer cross sections (MTCSs) were obtained from the DCSs by extrapolation of the DCSs to small and large θ and solid-angle integrating the DCSs as described in detail in earlier papers e.g. by Hargreaves *et al.*[68]

III. THEORY AND COMPUTATIONAL ASPECTS

To investigate the electronic excitation of benzene by electron scattering, we employed the SMC method, which is reviewed elsewhere.[69] The details concerning the target description and the electron scattering calculations are the same as presented in our recent paper about elastic scattering,[46] and here we summarize some key aspects that are necessary for the discussion of the results.

Three different basis sets (B1, B2, and B3) were employed, which contain progressively more diffuse basis functions and thus a denser set of higher-lying Rydberg states below ≈ 10 eV. The target electronic ground state was described at the Hartree-Fock level, whereas the excited states were described at the truncated configuration interaction singles (TCIS) level, introduced in Ref. 70. The set of single excitations is defined by two parameter, $\varepsilon_{\rm TCIS}$ and $N_{\rm pairs}$.[70] The first determines which are the relevant excited states for the TCIS, meaning that only the states with excitation energies below $\varepsilon_{\rm TCIS}$ are considered in the selection of excitations. Here we chose $\varepsilon_{\rm TCIS} = 10$ eV. $N_{\rm pairs}$ is the number of single excitations that are taken into account. Here, this parameter was chosen such that the TCIS Hamiltonian produced excitation energies only up to $\varepsilon_{\rm TCIS}$, which led to $N_{\rm pairs} = 58$, 152 and 218, for basis sets B1, B2 and B3, respectively.

The space of energetically accessible channels included all target states lying below a threshold value $\varepsilon_{\rm P}$ (which defines the projection operator in the SMC method). We explored two choices for $\varepsilon_{\rm P}$. In model A, we adopted $\varepsilon_{\rm P} = 9.09$ eV (corresponding to the first ionization potential of benzene using the Koopmanns' theorem), whereas in model B the value of $\varepsilon_{\rm P} = 10$ eV was taken. Notice that, since $\varepsilon_{\rm P} = \varepsilon_{\rm TCIS}$ in model B, all target states described at the corresponding TCIS level are treated as open channels. On the other hand, $\varepsilon_{\rm P} < \varepsilon_{\rm TCIS}$ in model A, meaning that the states between 9.09 and 10 eV are treated as closed channels in these calculations. The two choices for $\varepsilon_{\rm P}$ allow us to assess the impact of including states slightly above the first IP in calculating electronic excitation

cross sections, in this sense also extending our paper on elastic scattering,[46] where the same question was raised.

Table I summarizes the six scattering models and the number of configuration state functions (CSFs) that are used to expand the scattering wave function. For instance, the B3-B-437ch model corresponds to basis set B3 and multichannel coupling scheme B, giving rise to 437 open channels. Notice that results for two out of the six models were first presented in a preliminary publication,[36] which are reproduced here together with the results for the four other models. Thanks to algorithmic improvements, our code can now handle more than four hundred open channels for a system the size of benzene. In this sense, the present calculations are the most sophisticated ever performed with the SMC method in terms of number of coupled open channels (437), surpassing the previous record for a significantly smaller system, ethanol (431).[70] In addition, the present calculations account for five times more open channels than the latest set of SMC calculations for a molecule of similar size, *para*-benzoquinone (89).[39,42,71–73]

TABLE I. Summary of the six scattering models discussed in this work.

Basis set	$\varepsilon_P = 9.09$ eV	$\varepsilon_P = 10$ eV	#CSFs
B1	B1-A-099ch	B1-B-117ch[a]	19775
B2	B2-A-258ch	B2-B-305ch[a]	53281
B3	B3-A-315ch	B3-B-437ch	86939

[a] Results reported in Ref. 36 and reproduced here.

IV. RESULTS AND DISCUSSION

A. Electron energy loss spectrum

A sample of electron energy loss spectra obtained in the present measurements is shown in Fig. 1. The spectra were taken with the elastic scattering peak as was done in our work on CO.[51,52] The transmission of the spectra was determined by running a CO spectrum at the same E_0 values and correcting for the inelastic to elastic ratios from the time-of-flight spectra also measure in Ref. 51. Typical correction factors ranged from 1.78 at E_0 of 10 eV and 1.19 at E_0 of 20 eV. These spectra were obtained with the background subtracted using the gas beam in and out of the collision region, i.e. signal plus background and background spectrum, respectfully, taken concurrently. We found that the features I to III were separated and within an approximate conservative 20% error, we could demarcate the features as well as evaluate reasonable intensities for features IV and V as is shown in Fig. 1. This is unlike the situation reported in Kato *et al.*[27] who do not clearly discuss how they accounted for the significant background between their features I to V and caused them to unfold their spectra using multi-Gaussian bands. We also attempted to unfold the features using a multi-Gaussian unfolding program that was used for water spectra successfully conducted in our laboratory by Ralphs *et al.*[77] However, this was unsuccessful, showing wild deviations of over 100% as compared to the cursors' method previously discussed which was found to present not more than around 20% in uncertainty. Since in the background subtracted energy loss spectra the first 3 electronic features could be separated, we resorted to gas beam on spectra only to make our acquisition times twice as efficient, but now we fitted the background between the features I and II and between II and III by a visually guided linear or quadratic fit so that the background between I and II and between II and III was zero. We then integrated the counts (left over after subtraction of the background) using the cursors method. This was performed for energy loss areas of (I) 3.49 to 4.46 eV, (II) 4.46 to 5.32 eV, (III) 5.52 to 5.84 eV, (IV) 5.84 to 6.58 eV, and (V) 6.58 to 7.37 eV energy loss regions, approximately. After correction for transmission, the spectra were normalized to the elastic scattering DCSs of Cadena *et al.*,[46] which adds an approximate 12 to 13 % additional error, as is regularly done in such analysis.

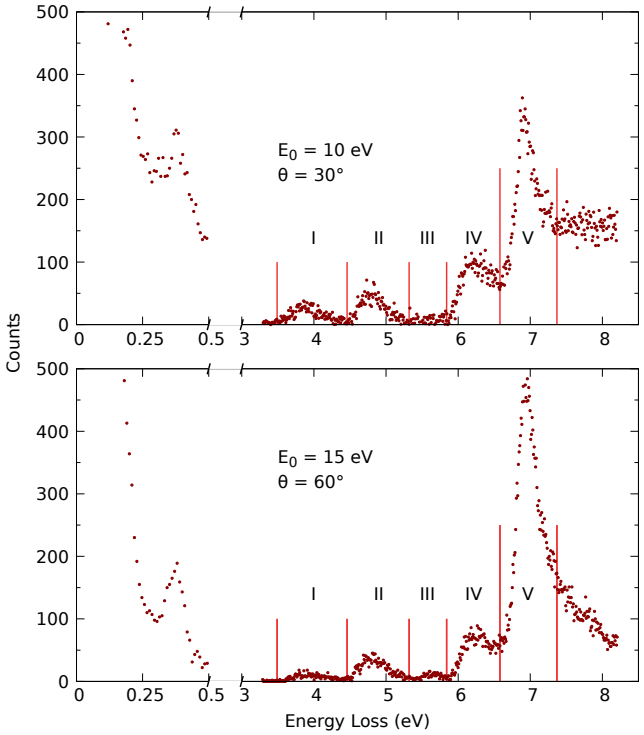

FIG. 1. Electron energy loss spectrum of benzene taken at $E_0 = 10$ eV and $\theta = 30^\circ$ (top), and at $E_0 = 15$ eV and $\theta = 60^\circ$ (bottom). The feature at around 0.38 eV corresponds to excitation of C−H stretching modes, whereas the vertical lines determine the intervals of each electronic excitation band, numbered from I to V.

B. Differential cross sections

The full set of experimental DCSs is presented in Fig. 2 and in Tables III, IV, V and VI, for the impact energies E_0 of 10, 12.5, 15 and 20 eV, respectively. The calculations were performed at the same energies, except for the lowest one, where we employed $E_0 = 10.5$ eV instead. This is because the TCIS

TABLE II. Vertical excitation energies (in eV) of benzene, according to experiment, EOM-CC3 and different TCIS calculations (see text for details).

Band	State	Dipole-allowed	Expt.[a]	EOM-CC3[b]	TCIS[c]	TCIS[d]	TCIS[e]
I	1^3B_{1u}		3.95	4.05	4.15	4.14	4.14
II	1^3E_{1u}		4.76	4.76	4.84	4.84	4.83
	1^1B_{2u}		4.90	4.97	6.00	5.99	5.99
III	1^3B_{2u}		5.60	5.75	5.54	5.53	5.53
IV	1^3E_{1g}		6.28	6.32	6.50	6.50	6.50
	1^1B_{1u}		6.20	6.38	6.75	6.71	6.71
	1^1E_{1g}		6.33	6.36	6.57	6.57	6.57
V	1^3A_{2u}			6.84	6.97	6.96	6.96
	1^3E_{2u}			6.95	7.12	7.11	7.10
	1^3A_{1u}			7.06	7.26	7.25	7.24
	2^3E_{1u}			7.11	7.14	7.12	7.12
	2^3E_{1g}			7.38	7.49	7.47	7.46
	1^3B_{1g}			7.54	7.67	7.67	7.65
	1^3B_{2g}			7.51	7.65	7.64	7.64
	1^3E_{2g}			7.34	7.77	7.75	7.74
	3^3E_{1g}			7.54	7.68	7.67	7.67
	1^1A_{2u}	yes	6.93	6.91	7.04	7.03	7.02
	1^1E_{1u}	yes	6.94	7.01	7.18	7.16	7.16
	1^1E_{2u}		6.95	6.97	7.13	7.12	7.12
	1^1A_{1u}			7.05	7.26	7.25	7.24
	2^1E_{1u}	yes	7.41	7.26	8.09	8.07	8.08
	2^1E_{1g}			7.46	7.56	7.55	7.54
	1^1B_{2g}			7.56	7.67	7.66	7.66
	1^1B_{1g}			7.54	7.68	7.66	7.66
	3^1E_{1g}			7.56	7.70	7.69	7.68

[a] Refs. 15–17, 74–76
[b] Ref. 36
[c] B1 basis set
[d] B2 basis set
[e] B3 basis set

calculations still generate states slightly above 10 eV, which are treated as open channels in the B models. The assignment of the states in bands I to V is presented in Table II, and is based on previous EOM-CC3 calculations.[36] In the following, we present and discuss the main features of each band separately, and then we explore in detail the results obtained with the scattering calculations.

Excitation of the lowest-lying excited state of benzene, 1^3B_{1u}, accounts for band I. The DCSs are shown in Fig. 3. Despite some angular features, the magnitudes do not vary much as a function of θ, which would be expected for excitation of triplet states.[78–80] For this particular band, the calculated DCSs at 10 eV lie systematically above the experimental data, even at intermediate angles ($\theta > 30^\circ$), which is not the case for the other bands.

Band II comprises the second lowest-lying triplet and the lowest-lying singlet states, 1^3E_{1u} and 1^1B_{2u}. The DCSs (presented in Fig. 4) are comparable in magnitude to those of band I, albeit usually somewhat larger (also see Fig. 2). In contrast to the more isotropic results for the lower lying band, the DCSs of band II tend to increase in the forward direction ($\theta < 30^\circ$), which becomes more prominent as a function of E_0. Forward peaking in the DCSs stems from electrons that deviated little from their income direction, meaning they passed far from the target and interacted only with the leading term of the long-range molecular potential. This is represented by the transition dipole moment in the case of electronic excitation. Electron-impact excitation accompanied by forward scattering is thus subject to the same spin and spatial selection rules as in optical spectroscopy.[81,82] While the peak observed in band II is the typical behavior for dipole-allowed transitions, the transition from the ground state to the 1^1B_{2u} state is dipole-forbidden. A vibronic coupling mechanism[83,84] reconciles these two observations, in the same way as it explains weak optical absorption bands.[85,86] Vibrations also participate during the electronic excitation, and the symmetries of the initial and final vibrational states must also be accounted for to establish whether the vibronic transition is dipole-allowed or not. Therefore, even though excitation of the 1^1B_{2u} state is dipole-forbidden at the equilibrium geometry, the transition may gain some intensity through vibrational modes (of appropriate symmetry) that couple it to dipole-allowed states from band V. The presently observed forward peak in band II strongly suggests that vibronic coupling plays a role in excitation of this band. This is also supported by calculations for the optical oscillator strengths of vibronic transitions,[87,88]

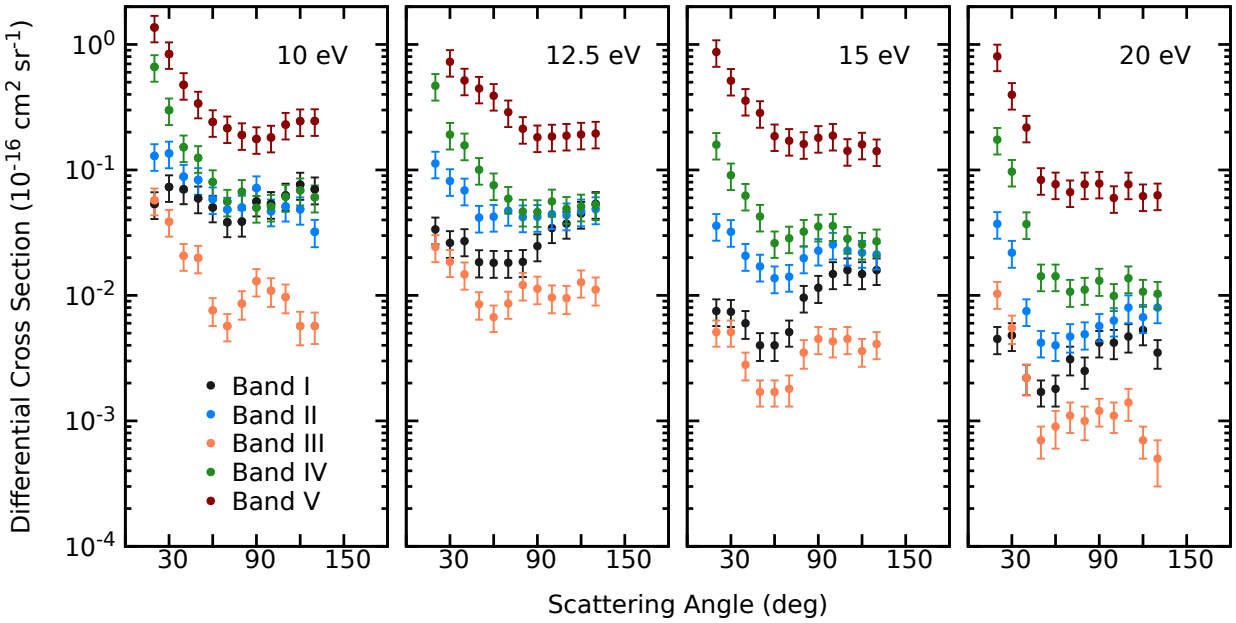

FIG. 2. Measured electron scattering differential cross sections for electronic excitation of the five lowest-lying electronic bands of benzene.

TABLE III. DCSs for the excitation to bands I to V, and to the fundamental composite vibrational stretching modes (ν_{str}), at $E_0 = 10$ eV, in units of 10^{-16}cm^{2}sr^{-1}, along with ICSs and MTCSs, in units of 10^{-16}cm^2, and their corresponding statistical errors. Values in parenthesis were obtained by extrapolation, as described in Section II.

θ (deg)	I	Error	II	Error	III	Error	IV	Error	V	Error	ν_{str}	Error
0	(0.03)		(0.16)		(0.1)		(2.)		(3.5)		(0.1)	
5	(0.035)		(0.15)		(0.085)		(1.5)		(2.5)		(0.1)	
10	(0.04)		(0.14)		(0.075)		(1.2)		(2.)		(0.1)	
20	0.053	0.013	0.13	0.03	0.057	0.014	0.66	0.16	1.4	0.3	0.10	0.03
30	0.073	0.018	0.14	0.03	0.039	0.009	0.30	0.07	0.84	0.20	0.11	0.03
40	0.070	0.017	0.089	0.021	0.021	0.005	0.15	0.04	0.48	0.11	0.087	0.021
50	0.059	0.014	0.083	0.020	0.020	0.005	0.12	0.03	0.34	0.08	0.095	0.023
60	0.050	0.012	0.059	0.014	0.0076	0.0019	0.080	0.019	0.24	0.06	0.091	0.022
70	0.038	0.009	0.048	0.012	0.0057	0.0014	0.056	0.013	0.22	0.05	0.10	0.02
80	0.039	0.009	0.050	0.012	0.0086	0.0022	0.067	0.016	0.19	0.05	0.11	0.03
90	0.056	0.014	0.072	0.017	0.013	0.003	0.050	0.012	0.18	0.04	0.12	0.03
100	0.054	0.013	0.047	0.011	0.011	0.003	0.051	0.012	0.18	0.04	0.12	0.03
110	0.063	0.015	0.051	0.012	0.0097	0.0025	0.061	0.015	0.23	0.06	0.13	0.03
120	0.076	0.019	0.048	0.012	0.0057	0.0017	0.069	0.017	0.24	0.06	0.12	0.03
130	0.070	0.017	0.032	0.008	0.0057	0.0016	0.061	0.015	0.25	0.06	0.12	0.03
140	(0.065)		(0.027)		(0.0045)		(0.06)		(0.22)		(0.11)	
150	(0.06)		(0.024)		(0.004)		(0.065)		(0.25)		(0.105)	
160	(0.055)		(0.022)		(0.0035)		(0.065)		(0.25)		(0.11)	
170	(0.05)		(0.021)		(0.003)		(0.065)		(0.27)		(0.11)	
180	(0.05)		(0.02)		(0.0027)		(0.065)		(0.29)		(0.11)	
ICS	0.722	0.184	0.744	0.190	0.166	0.044	1.493	0.380	4.186	1.062	1.388	0.353
MTCS	0.745	0.187	0.563	0.141	0.100	0.026	0.839	0.210	2.960	0.737	1.440	0.359

found to be larger in those involving the ν_{18} ring deformation mode. Here, the vibrational modes are numbered according to Herzberg's convention.[89]

Our scattering calculations do not reproduce the weak forward peak of band II, for two reasons. First, being a fixed-nuclei calculation, it ignores the vibrational motion, and consequently cannot describe the vibronic coupling. Second, the use of square-integrable Gaussian basis functions in the SMC method effectively truncates the long-range potential that mediates the excitation. In turn, our calculations are expected to be more accurate for scattering at larger scattering angles ($\theta > 30^\circ$), governed by short-range interactions between the electron and the target molecule. They show, for instance, that excitation of the degenerate 1^3E_{1u} triplet state amounts to

TABLE IV. As in Table III, but for $E_0 = 12.5$ eV.

θ (deg)	I	Error	II	Error	III	Error	IV	Error	V	Error	ν_{str}	Error
0	(0.055)		(0.2)		(0.040)		(0.8)		(5.)		(0.04)	
5	(0.050)		(0.17)		(0.035)		(0.7)		(4.)		(0.04)	
10	(0.040)		(0.14)		(0.030)		(0.6)		(3.)		(0.04)	
20	0.034	0.008	0.11	0.03	0.024	0.006	0.47	0.11	2.03	0.48	0.041	0.010
30	0.026	0.006	0.082	0.020	0.018	0.004	0.19	0.05	0.73	0.17	0.041	0.010
40	0.027	0.007	0.069	0.016	0.015	0.004	0.16	0.04	0.52	0.12	0.043	0.010
50	0.018	0.004	0.042	0.010	0.008	0.002	0.10	0.02	0.45	0.11	0.035	0.008
60	0.018	0.004	0.042	0.010	0.007	0.002	0.076	0.018	0.39	0.09	0.032	0.008
70	0.018	0.004	0.047	0.011	0.009	0.002	0.059	0.014	0.29	0.07	0.037	0.009
80	0.019	0.004	0.042	0.010	0.012	0.003	0.047	0.011	0.21	0.05	0.038	0.009
90	0.025	0.006	0.042	0.010	0.011	0.003	0.046	0.011	0.18	0.04	0.042	0.010
100	0.034	0.008	0.044	0.011	0.010	0.002	0.056	0.013	0.18	0.04	0.058	0.014
110	0.037	0.009	0.043	0.010	0.010	0.002	0.049	0.012	0.19	0.04	0.061	0.015
120	0.045	0.011	0.047	0.011	0.013	0.003	0.051	0.012	0.19	0.05	0.062	0.015
130	0.054	0.013	0.049	0.012	0.011	0.003	0.053	0.013	0.20	0.05	0.072	0.017
140	(0.060)		(0.048)		(0.011)		(0.06)		(0.2)		(0.076)	
150	(0.065)		(0.05)		(0.011)		(0.065)		(0.2)		(0.08)	
160	(0.070)		(0.05)		(0.011)		(0.07)		(0.2)		(0.085)	
170	(0.075)		(0.05)		(0.011)		(0.07)		(0.2)		(0.09)	
180	(0.080)		(0.05)		(0.011)		(0.07)		(0.2)		(0.1)	
ICS	0.436	0.112	0.650	0.165	0.146	0.038	1.160	0.295	4.763	1.207	0.654	0.167
MTCS	0.534	0.135	0.587	0.147	0.135	0.035	0.756	0.189	2.815	0.701	0.763	0.191

TABLE V. As in Table III, but for $E_0 = 15$ eV.

θ (deg)	I	Error	II	Error	III	Error	IV	Error	V	Error	ν_{str}	Error
0	(0.009)		(0.04)		(0.006)		(0.25)		(2.)		(0.015)	
5	(0.009)		(0.038)		(0.0055)		(0.22)		(1.7)		(0.015)	
10	(0.0085)		(0.038)		(0.0055)		(0.19)		(1.4)		(0.015)	
20	0.0075	0.0018	0.036	0.009	0.0051	0.0012	0.16	0.04	0.87	0.21	0.014	0.003
30	0.0074	0.0018	0.032	0.008	0.0051	0.0012	0.091	0.022	0.51	0.12	0.013	0.003
40	0.0060	0.0015	0.021	0.005	0.0028	0.0007	0.062	0.015	0.36	0.09	0.011	0.003
50	0.0040	0.0010	0.017	0.004	0.0017	0.0004	0.042	0.010	0.28	0.07	0.009	0.002
60	0.0040	0.0010	0.014	0.003	0.0017	0.0004	0.026	0.006	0.19	0.04	0.006	0.002
70	0.0051	0.0012	0.014	0.003	0.0018	0.0005	0.029	0.007	0.17	0.04	0.009	0.002
80	0.0096	0.0023	0.020	0.005	0.0035	0.0009	0.032	0.008	0.16	0.04	0.008	0.002
90	0.011	0.003	0.023	0.005	0.0045	0.0011	0.035	0.008	0.18	0.04	0.008	0.002
100	0.015	0.004	0.025	0.006	0.0043	0.0011	0.036	0.009	0.19	0.04	0.012	0.003
110	0.016	0.004	0.023	0.005	0.0045	0.0011	0.028	0.007	0.14	0.03	0.010	0.002
120	0.015	0.004	0.022	0.005	0.0036	0.0009	0.025	0.006	0.16	0.04	0.012	0.003
130	0.016	0.004	0.021	0.005	0.0041	0.0010	0.027	0.006	0.14	0.03	0.012	0.003
140	(0.0159)		(0.02)		(0.004)		(0.03)		(0.135)		(0.013)	
150	(0.0158)		(0.018)		(0.004)		(0.03)		(0.13)		(0.013)	
160	(0.0155)		(0.017)		(0.0035)		(0.033)		(0.125)		(0.013)	
170	(0.015)		(0.016)		(0.0035)		(0.035)		(0.12)		(0.013)	
180	(0.015)		(0.015)		(0.0035)		(0.035)		(0.135)		(0.013)	
ICS	0.137	0.035	0.265	0.067	0.045	0.012	0.529	0.134	2.979	0.755	0.134	0.034
MTCS	0.167	0.042	0.257	0.064	0.047	0.012	0.397	0.099	2.048	0.510	0.139	0.035

$\approx 80\%$ of the DCSs of band II at $E_0 = 10.5$ eV, decreasing to $\approx 50\%$ at $E_0 = 50$ eV, the expected trend for the short-range exchange interaction responsible for excitation of triplets.

Band III stems from excitation of the third lowest-lying triplet state, 1^3B_{2u}. The DCSs, shown in Fig. 5, are the smallest of the five bands, being considerably smaller than those of the lower-lying triplets, from bands I and II (see Fig. 2). Excitation of this triplet state is accompanied by a surprising increase of the DCS at small θ, resembling more the results of band II (dominated by a singlet) than of band I (a single triplet). This is unexpected because spin-forbidden transitions require short-range interactions, whereas scattering at small θ is governed by the long-range Coulombic potential (which precludes singlet-triplet excitation). Band III is well separated in energy from its neighbouring bands, such that spurious contributions from other states can be ruled out. While a vibronic

TABLE VI. As in Table III, but for $E_0 = 20$ eV.

θ (deg)	I	Error	II	Error	III	Error	IV	Error	V	Error	ν_{str}	Error
0	(0.006)		(0.1)		(0.06)		(0.4)		(2.)		(0.12)	
5	(0.0055)		(0.08)		(0.045)		(0.35)		(1.5)		(0.10)	
10	(0.005)		(0.06)		(0.03)		(0.3)		(1.2)		(0.07)	
20	0.0045	0.0011	0.037	0.009	0.010	0.003	0.17	0.04	0.80	0.19	0.043	0.018
30	0.0048	0.0012	0.022	0.005	0.0055	0.0014	0.097	0.023	0.40	0.09	0.024	0.006
40	0.0022	0.0006	0.0075	0.0018	0.0022	0.0006	0.037	0.009	0.22	0.05	0.025	0.006
50	0.0017	0.0004	0.0042	0.0010	0.00074	0.00021	0.014	0.003	0.083	0.020	0.013	0.003
60	0.0018	0.0005	0.0040	0.0010	0.00090	0.00026	0.014	0.003	0.077	0.018	0.010	0.003
70	0.0031	0.0008	0.0047	0.0012	0.0011	0.0003	0.011	0.003	0.067	0.016	0.007	0.002
80	0.0025	0.0007	0.0049	0.0012	0.00096	0.00027	0.011	0.003	0.077	0.018	0.010	0.002
90	0.0042	0.0010	0.0057	0.0014	0.0012	0.0003	0.013	0.003	0.078	0.019	0.016	0.004
100	0.0042	0.0011	0.0063	0.0016	0.0011	0.0003	0.0099	0.0024	0.060	0.014	0.013	0.003
110	0.0047	0.0012	0.0080	0.0020	0.0014	0.0004	0.014	0.003	0.077	0.018	0.017	0.004
120	0.0053	0.0013	0.0067	0.0017	0.00072	0.00024	0.011	0.003	0.062	0.015	0.021	0.005
130	0.0035	0.0009	0.0080	0.0020	0.00053	0.00018	0.010	0.003	0.063	0.015	0.018	0.004
140	(0.003)		(0.008)		(0.0004)		(0.01)		(0.06)		(0.017)	
150	(0.0025)		(0.0085)		(0.00045)		(0.01)		(0.07)		(0.015)	
160	(0.002)		(0.009)		(0.0005)		(0.01)		(0.07)		(0.015)	
170	(0.002)		(0.0095)		(0.0005)		(0.01)		(0.07)		(0.013)	
180	(0.002)		(0.01)		(0.0005)		(0.01)		(0.075)		(0.011)	
ICS	0.043	0.011	0.112	0.029	0.025	0.007	0.332	0.085	1.688	0.428	0.213	0.055
MTCS	0.044	0.012	0.090	0.023	0.011	0.003	0.155	0.039	0.930	0.232	0.194	0.049

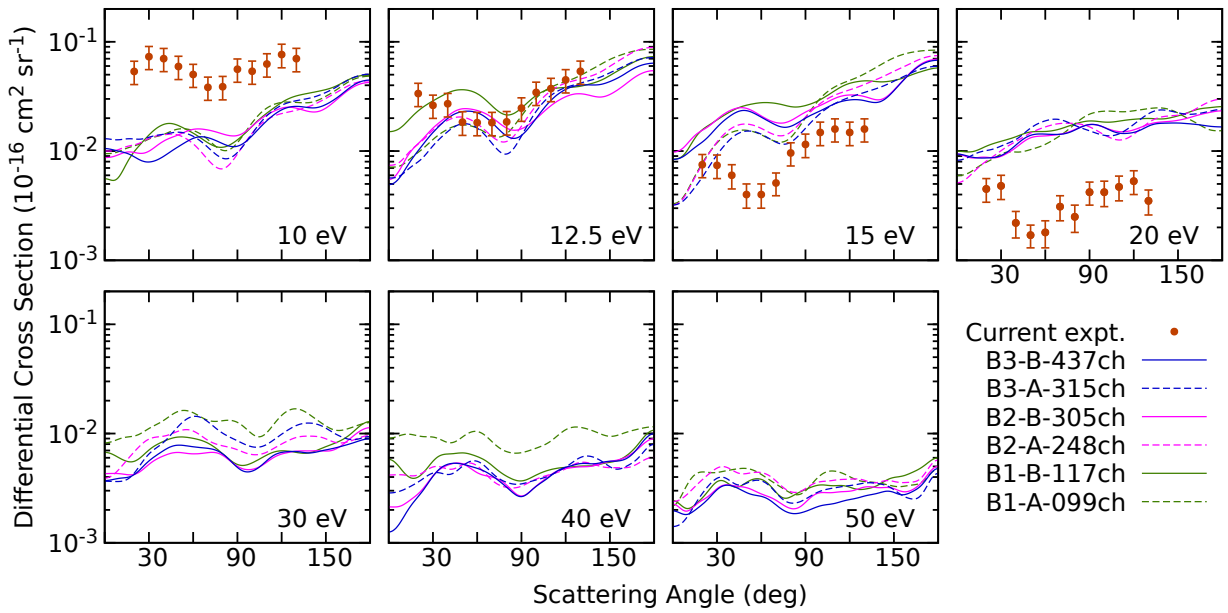

FIG. 3. Electron scattering differential cross sections for electronic excitation of band I of benzene, according to our current measurements and our six scattering models. The B1-B-117ch and B2-B-305ch results were first reported in Ref. 36.

coupling effect may play a role, it alone cannot account for the observed forward peak. For that, either there is a short-range mechanism that favors the forward scattering or there is a long-range mechanism that mediates such spin-flip transition. At present, the mechanism underlying this weak though apparent forward peak is unclear, but we believe the present observation will encourage future theoretical attempts to clarify it.

Three states contribute to band IV, 1^3E_{1g}, 1^1B_{1u} and 1^1E_{1g}. The DCSs for excitation of this band are presented in Fig. 6, together with the experimental data reported by Kato *et al.*[27] They display larger magnitudes than those of the three lower-lying bands (see Fig. 2). Whereas both measurements provide comparable results at 15 eV, the present DCSs are significantly larger than the previous ones[27] at 10 eV for $\theta < 60°$. We come back to this point later when discussing similar dis-

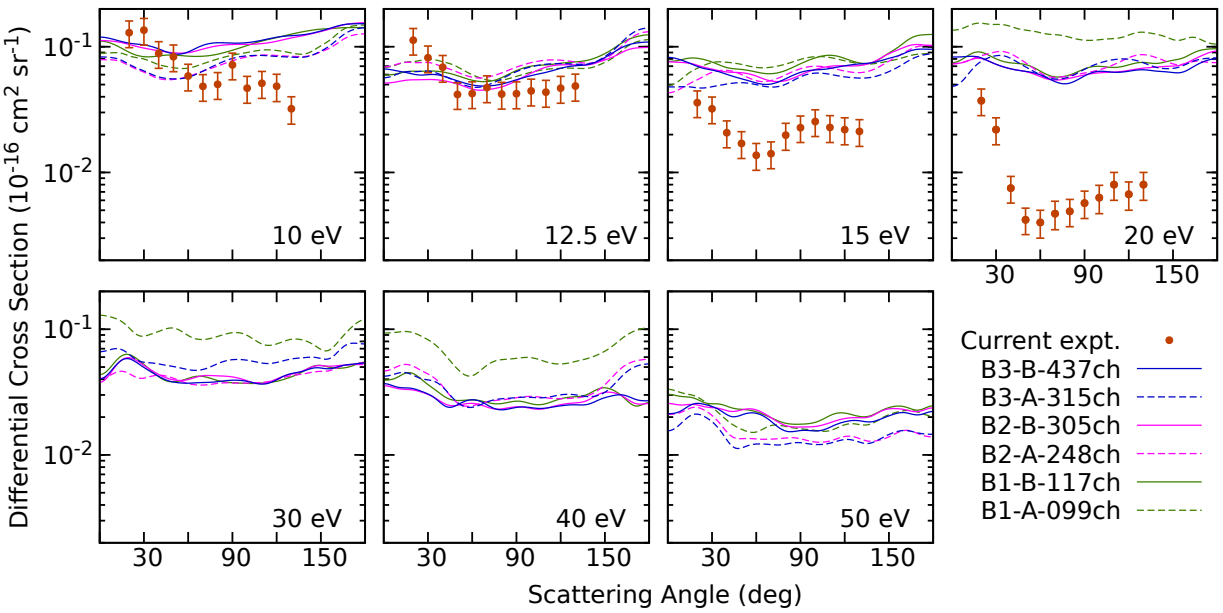

FIG. 4. As in Fig. 3, but for band II.

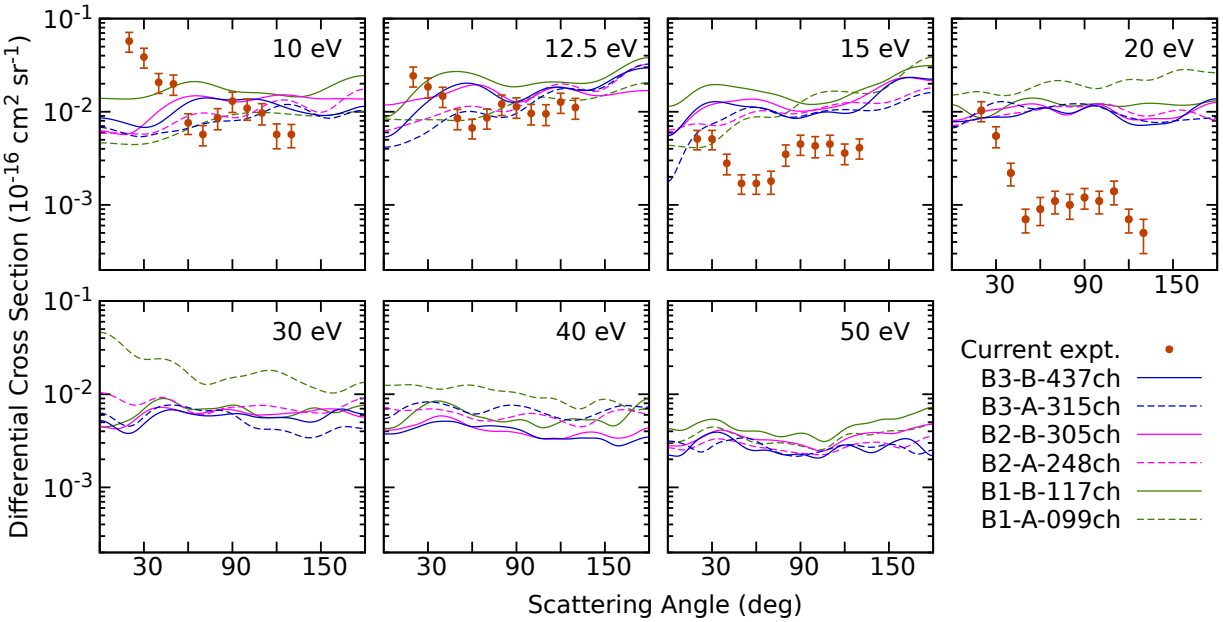

FIG. 5. As in Fig. 3, but for band III.

crepancies for band V. The DCSs of band IV are clearly forward peaked. Vibronic transitions would explain this feature, as already point out above for band II. In addition, the proximity between the states of band IV with the dipole-allowed states of band V favors their vibronic couplings and can explain the more pronounced forward peak displayed by this band, when compared to the weaker one in band II. This is consistent with the existing calculations for the optical oscillator strengths for vibronic transitions in bands IV and II,[87,88] which also showed that the former is dominated by excitation of the ν_{17} C−H bending mode. Our scattering calculations indicates that the contribution of the 1^1B_{1u} state to this band varies from an average of $\approx 20\%$ at $E_0 = 10.5$ eV to $\approx 60\%$ at $E_0 = 50$ eV.

Band V contains many more excited states than the lower-lying bands, all listed in Table II. The DCSs, shown in Fig. 7 have by far the largest magnitudes among the five bands, more clearly seen in Fig. 2. Significant discrepancies between the present experimental data and those from Kato *et al.*[27] can already be observed at 15 eV, becoming much more evident at

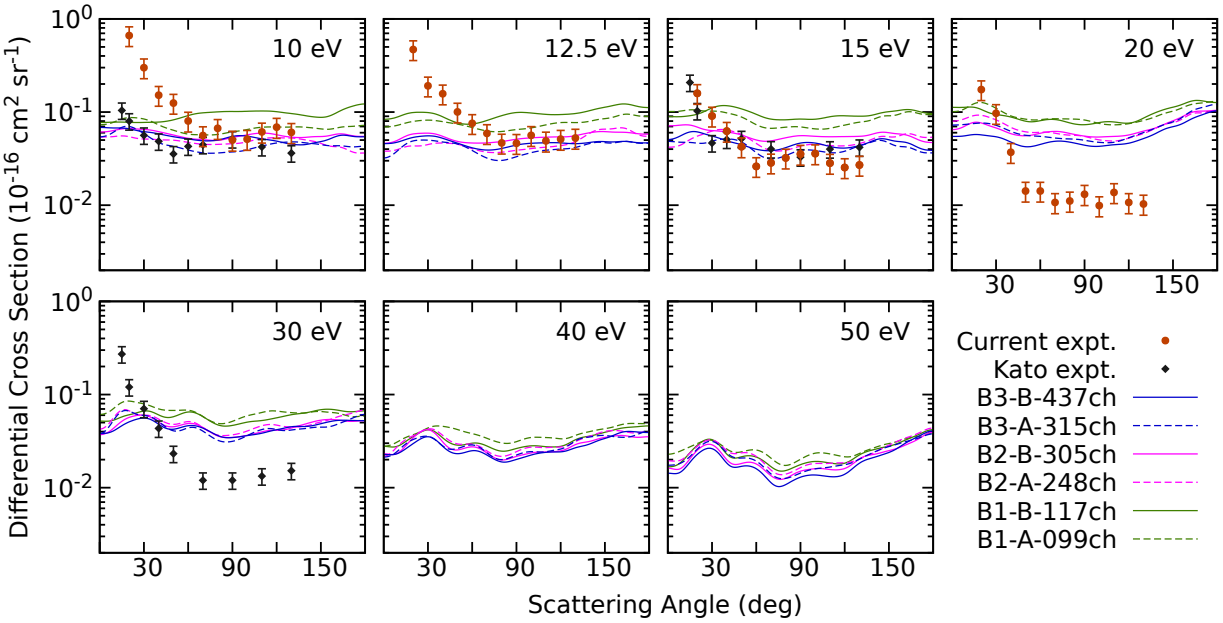

FIG. 6. As in Fig. 3, but for band IV, together with the available data from Kato *et al.*[27]

10 eV. Certainly, one can expect an increase in the DCSs for forward scattering based on the dipole-allowed transitions of this band (namely to the 1^1A_u, 1^1E_{1u} and 2^1E_{1u} states), which turns out to be much more pronounced in the present work than in the report by Kato *et al.*[27]

We have considered possible explanations for such important differences observed for band IV and (most noticeably) band V. They could be related to instrumental transmission factors, which need to be corrected to standards such as helium ionization[90] or time-of-flight spectroscopy.[51,52] This would be especially relevant at the low residual electron energies (≈ 3 eV) associated with this excitation at E_0 of 10 eV. However, both Kato *et al.* and this work take into consideration transmission aspects, so that is probably not the reason. Two significant instrumental differences between the two experiments concern the energy resolution as well the angular resolution, better by almost a factor of two in the earlier work.[27] However, all the main features are well separated and resolved in the present energy loss spectra, such that our energy resolution should be sufficient. Similarly, there is no reason to believe that differences in the angular resolution would produce the observed discrepancies. Furthermore, the comparison between the two experimental data sets do not indicate any obvious possible systematic errors. From the theoretical side, a fixed-nuclei scattering calculation could in principle describe the forward peak of band V, since its underlying transitions are dipole-allowed. However, as pointed out in the discussion of band II, the use of Gaussian basis function in our current SMC implementation hampers the description of the long-range potential that induces the dipole-allowed transitions. Instead, we explored the first Born approximation applied to the dipole potential to compute the DCSs for the three dipole-allowed transitions of band V. Even though they present the characteristic forward peak, their magnitudes are too big by one or two orders of magnitude relative to the present measurements. For such strong dipole-allowed transitions and relatively low E_0, this dipole-Born approximation showed to be unreliable.[91] In turn, the SMC calculations are expected to become accurate at intermediate θ, in comparison to the small θ regime. Indeed, for intermediate θ and at $E_0 =$ 10 eV, our calculations produce fairly good DCSs for excitation of bands II, III, and IV (less so for band I), in view of the agreement with the present and the previous experiments.[27] Assuming the calculations are similarly accurate for band V, the comparison (see Fig. 7) would be in favor of the presently reported DCSs. Moreover, as will be shown later, the present DCSs for vibrational excitation of the C−H stretching modes is in very good agreement with previous measurements from Allan *et al.*,[92] which gives some reassurance to the present measurements. These indications are not conclusive though, and the cause of the difference between the two experimental results remains unclear at present. All in all, there is no *a priori* fundamental reason to tell which experiment produced DCSs closer to the true values. Further experimental investigations are clearly needed to shed light on the small θ, low E_0 DCSs for bands IV and V.

Excitation of band V at small θ is expected to be dominated by the three dipole-allowed transitions, to the 1^1A_{2u}, 1^1E_{1u} and 2^1E_{1u} states, whereas the SMC calculations can reveal the specific contributions from each of the numerous underlying states for $\theta > 60^\circ$. For this analysis, we employed the computed ICSs (to be presented later) as a proxy, since the corresponding DCSs miss the forward peak and do not display marked angular features. We found that most states contribute between around 2 and 5 % to the ICSs of the band, no state accounting for less than 1%. An equal share would represent 3.6 %. This relatively equal share of excitation induced by electron impact stands out in striking contrast to the spin and

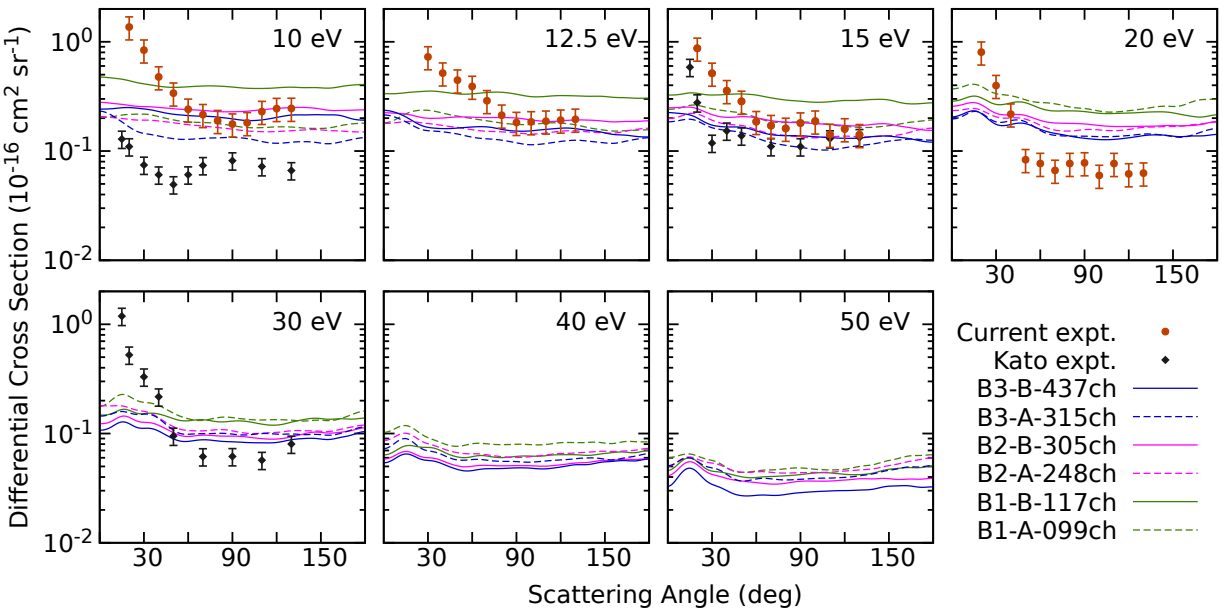

FIG. 7. As in Fig. 6, but for band V.

spatial selection rules of optical excitation. In a first approximation, the present results show that the short-range forces, which govern scattering at intermediate θ, induce excitation of all the 28 states of band V, irrespective of their character. With contributions ranging from 4 to 8%, the states with the overall largest cross sections are the 1^1A_{2u}, 1^1E_{1u} and 2^1E_{1u}, precisely the three optically bright states of band V. Therefore, there is still some preference for the dipole-allowed transitions, even at intermediate θ. This is surprising because dipole-allowed transitions would only be expected to dominate at small θ, controlled by the long-range interaction. The above findings are relatively independent of E_0.

Except for the current limitations of our theoretical models to describe scattering at small θ, as discussed above, the calculated DCSs agree reasonably well with the present experiment at 10 and 12.5 eV. However, they do not decrease as steeply as a function of E_0, appearing overestimated at 15 and specially at 20 eV. This growing discrepancy probably reflects the increasing number of open channels, ignored in our scattering calculations, which only accounts for the target states below $\approx$ 10 eV. We recall that our calculations were designed to account for as many Rydberg states as possible, in order to better understand their impact in the calculated electronic excitation cross sections (discussed below). Overestimated electronic excitation DCSs at higher energies have been observed in recent SMC calculations for *para*-benzoquinone[39,72] and ethanol[70] and would also be expected here.

In a previous theoretical investigation about electronic excitation of benzene,[36] we addressed how improving the description of the lower-lying target states, particularly the Rydberg states, impacted the computed DCSs. Relevant insights about this question are reported here, by extending the calculations from two[36] to six scattering models, by comparing with the presently measured DCSs for the five bands, and by performing a more in-depth analysis of the results. Augmenting the basis set from B2 to B3 increases the number of higher-lying Rydberg states in the $\approx$ 7 to 10 eV region, causing the DCSs to typically decrease, continuing the trend that was observed when enlarging from the B1 to the B2 basis set.[36] (In light of the results obtained with the B3 basis set and the more divergent behavior of the B1-A-099ch and B1-B-117ch models, basis set B1 can likely be considered too small.) An effect of similar order occurs when moving from models A to B, i.e. by treating the states between 9.09 and 10 eV (lying just above the first ionization threshold) as open channels in the calculations, often in the sense of also decreasing the DCSs. Similarly to what has been found for elastic scattering,[46] the magnitudes of the DCSs for excitation of bands I, II and III are fairly well converged with respect to inclusion of Rydberg states. The same cannot yet be concluded for bands IV and V. Despite the clear importance of accounting for higher-lying Rydberg states in the calculations, there are still major differences between our most accurate scattering model (B3-B-437ch) and the experimental data, for all bands, most noticeably at higher energies. This highlights the need to account for target states above the ionization threshold, including the continuum states associated to ionization, in order to attain more quantitative electronic excitation DCSs covering a wide energy range. Explicitly accounting for the ionization channels represents a major long-term theoretical and computational challenge for the SMC method. As a short-term perspective, we are working on a model potential that attempts to mimic the effect of the ionization channels on the computed elastic and electronic excitation cross sections. Once this is finished, we plan to perform new calculations on electron scattering from benzene.

Improving the scattering models by accounting for more Rydberg states and by treating them as open channels affects

the computed DCSs of the five bands to different extents. In the scale of the experimental-theoretical comparison, the impact is relatively minor for bands I and II, becoming somewhat more relevant for band III. The three lower-lying bands comprise valence excitations only. In turn, the DCSs for excitation of bands IV and V decrease more substantially. By inspecting how the specific contributions to the DCSs of band IV behave as more higher-lying Rydberg states are accounted for, we found that the reduction stems mostly from the $\pi \rightarrow 3s$ Rydberg states, 1^3E_{1g} and 1^1E_{1g}, and to a far lesser extent from the $\pi \rightarrow \pi^*$ valence state, 1^1B_{1u}. As for band V, the DCSs for excitation of all states decrease, though to varying degrees. In relative terms, the states involving $\pi \rightarrow 3p_1$ transitions are most affected (p_1 means the Rydberg orbital is coplanar to the benzene ring), particularly the triplet states, 1^3A_{2u}, 1^3E_{2u} and 1^3A_{1u}. The $\pi \rightarrow 3p_0$ state, 1^3A_{1u}, is the least affected one (p_0 means the Rydberg orbital is perpendicular to the benzene ring), followed by the $\pi \rightarrow \pi^*$ valence states, 1^3E_{2g} and 1^1E_{2u}. The remaining excitations, of $\pi \rightarrow 3d$ character, lie in-between. Our analysis demonstrates that the higher-lying Rydberg states display strong multichannel coupling with the lower-lying Rydberg states of $3s$ and $3p_1$ character, but not with the $3p_0$ Rydberg and valence excited states. This explains the artificially large cross sections for excitation of $3s$ and $3p_1$ Rydberg states when decay to higher-lying Rydberg states are not allowed in the calculations.

C. Integral cross sections

The comparison between experimental and the set of theoretical ICSs for excitation of bands I to V are shown in Fig. 8, which also includes the available experimental data from Kato *et al.*[27] for bands IV and V and their calculated BE f-scaled ICSs for band V.[27] Following our discussion about the DCSs, the ICSs for bands IV and V are qualitatively different in the two experiments, steeply decreasing as a function of E_0 in the current measurements (just as for the lower lying bands), and being relatively constant (band IV) and even increasing with E_0 (band V) according to Kato *et al.*[27] Our calculations reproduce the decreasing ICSs as a function of E_0 observed in the present experiment, though considerably more gradually, as already pointed out in the discussion about the DCSs. For band V, the behavior is markedly distinct to the results obtained with BE f-scaled calculations,[27] which in turn is very close to the measurements performed in this same study. We further notice that the presently measured electronic excitation cross section (including up to band V) is exceeded by the ionization cross section between 15 eV and 20 eV (see Ref. 40 and references therein), which is consistent with the cross section data set reported in Ref. 40.

The relative excitation of the five bands can be appreciated more clearly in Fig. 9, which shows the ICSs for all bands, according to the current measurements and our most accurate scattering model (B3-B-437ch). Electronic excitation of band V dominates by far. The ICSs become progressively smaller for bands IV, II, I and III. The calculations are overall able to reproduce this important trend, except for the inverted positions of bands IV and II. To a great extent, this inversion stems from the missing forward peak of band IV and the particularly overestimated DCSs of band II in our calculations. While the trend is preserved across the different scattering models, the individual cross sections are impacted differently, as can be seen in Fig. 8. We found quite comparable ICSs for bands I and II, less so for band III, and more marked differences for band IV and V, which can be traced back to our previous discussion about the stronger couplings between the $3s$ and $3p_1$ Rydberg states of the latter two bands with the higher-lying Rydberg states.

D. Vibrational excitation of the fundamental C−H stretching modes

We also measured the vibrational excitation of the combined sum of the ν_1, ν_5, ν_{12} and ν_{15} C−H stretching modes of benzene at the mean energy loss value of ≈ 0.38 eV. Details about these modes can be found in Ref. 93. The four stretching modes grouped together as ν_{str} have the following energies and relative optical infrared intensities (in parentheses), ν_{15}: 0.376 eV (4.8), ν_1: 0.380 eV (10.6), ν_5: 0.380 eV (inactive) and ν_{12}: 0.384 eV (< 1).[93] This ν_{str} energy loss peak is resolved from the elastic one and its DCSs were determined after similarly normalizing it using the elastic DCSs of Cadena *et al.*[46] This is an added item to the main theme of electronic excitation.

Fig. 10 shows the DCSs for excitation of the ν_{str} stretching modes. There is very good agreement between our data at 10 and 12.5 eV and the DCSs measured at 90° by Allan *et al.*[92] while some small discrepancy is found at 15 eV. In the context of our previous discussion about the important discrepancies between the present measurements and those of Kato *et al.*[27] regarding bands IV and V, it is worth stressing such a good level agreement between the present measurements and those of Allan *et al.*[92] for excitation of the ν_{str} modes.

The overall DCSs decrease with E_0 in general. Essentially isotropic angular behavior of the vibrational excitation DCSs is seen at lower E_0 values. However, a non-isotropic forward-scattering angular behavior is observed at our highest E_0 of 20 eV. The DCSs trend towards more forward scattering angular behavior at higher E_0, similar to the excitation of the $a^3\Pi$ state of CO,[51] and similar to excitation of the analogous ν_{str} stretching modes in phenol,[94] pyrimidine,[95] and para-benzoquinone.[71] We hope the present DCSs will instigate further theoretical modeling of the excitation of these ν_{str} vibrational modes.

V. CONCLUSIONS

We have presented new experimental and theoretical electron scattering DCSs for the excitation of the lowest-lying five electronic excitation features of benzene at low E_0 values, along with experimental DCSs for the prominent stretching modes at 0.38 eV energy loss. The present contribution contains the first set of experimental DCSs for the three lower-

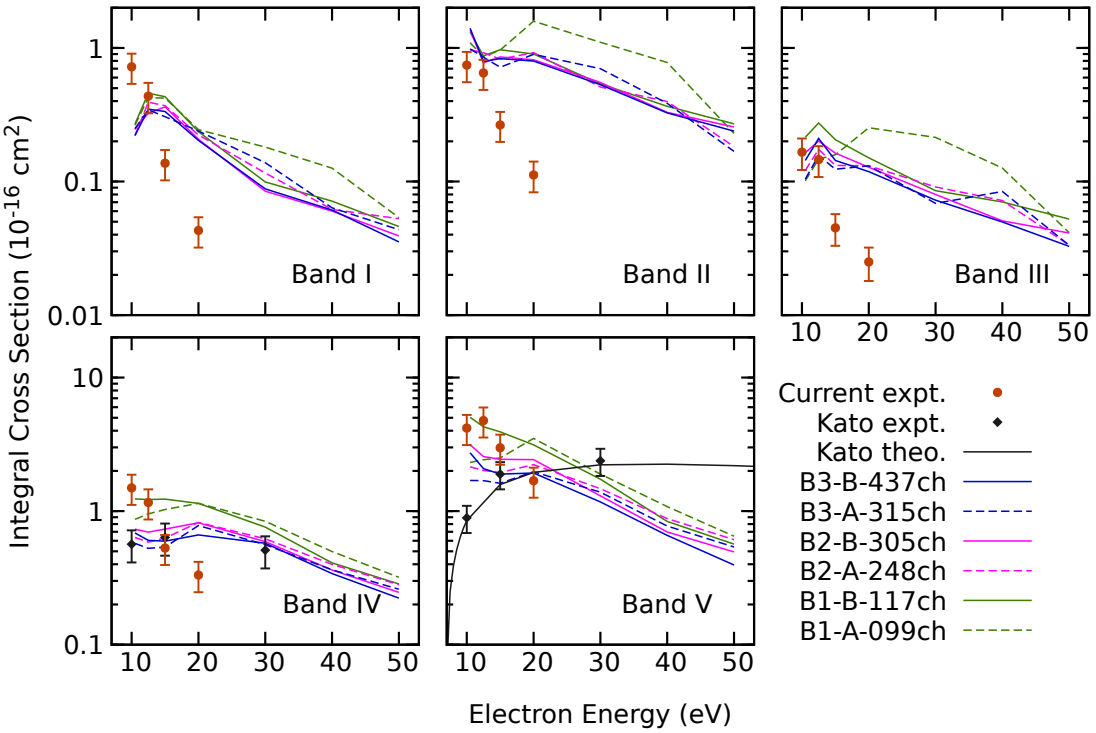

FIG. 8. Integral cross sections for electron impact electronic excitation of the bands I to V of benzene, according to our six scattering models, current measurements and previous measurements and calculations from Kato *et al.*[27] B1-B-117ch and B2-B-305ch results were first reported in Ref. 36.

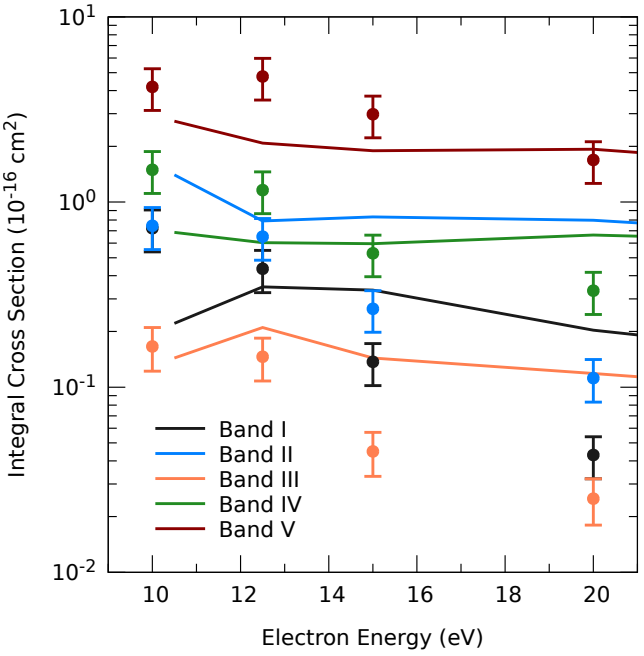

FIG. 9. Integral cross sections for electron impact electronic excitation of the lowest-lying five electronic bands of benzene, according to our most accurate scattering model, B3-B-437ch (solid line), and to the current measurements (dots).

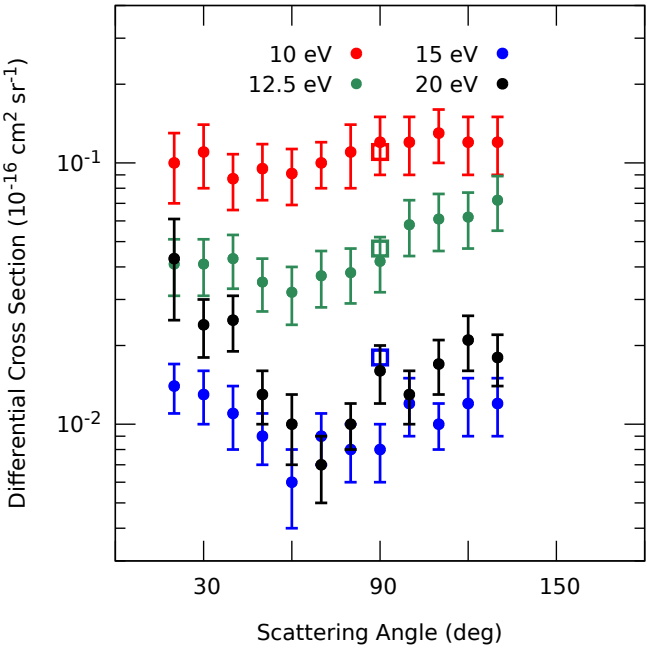

FIG. 10. DCSs for the electron impact vibrational excitation of the composite stretching modes ν_{str} of benzene at E_0 of 10, 12.5, 15 and 20 eV. Data from Allan *et al.*[92] for the three lower energies are indicated by open squares.

lying bands, and also supplements the earlier work of Kato *et al.*,[27] which covered only features IV and V. Despite the fair agreement between the two experiments at larger θ and higher E_0, we found a contrasting picture concerning small θ and lower E_0. We argue that there is no self-evident reason to claim the superiority of one set of measurements over the other. We notice, however, that the present experiments seem to agree better with the SMC calculations and also produce DCSs for vibrational excitation of the ν_{str} modes in very good agreement with measurements of Allan *et al.*[92] Repeated and more differential scattering work is required to clarify the observed discrepancies. Overall, our experimental results are in decent agreement with theory for such a challenging molecule. Agreement improves at intermediate θ and lower E_0 and deteriorates at smaller θ and higher E_0, which is related to the limited description of long-range interactions and the missing ionization channels in our model, respectively. As such, our calculated cross sections should be increasingly less quantitative towards higher energies, which is confirmed by the experiment. The largest errors, of around one order of magnitude, are seen at 20 eV (the highest energy probed in our experiment), whereas larger errors would be expected at higher energies, where the ionization channel prevails. In the future, theoretical models will need to address the continuum of ionization channels and the long-range interactions more accurately.

We have discussed how our theoretical and experimental results provide a series of interesting insights about the dynamics of electron-benzene collisions. The forward peak observed in bands II and IV, which do not have dipole-allowed transitions, clearly indicates the involvement of vibronic couplings mediated by the long-range potential. A similar but totally unexpected forward peak was also observed for band III, which arises from a single spin-forbidden transition. The origin of this feature is not clear. Moving to band V, the most intense one, the calculations showed that all its 28 underlying states have a comparable share of the cross sections at intermediate θ. In other words, the short-range interaction excites all these electronic states rather indistinctly. Despite some preference for the three dipole-allowed transitions, the larger fraction of the cross section stems from the summed contribution from the dipole-forbidden transitions. Furthermore, our calculations allowed us to comprehensively explore the effect of higher-lying Rydberg states in the electronic excitation of the lower-lying bands. We found their influence to be major for the calculated excitation cross sections of the lower-lying Rydberg states of $3s$ and $3p_1$ character, mild for those of the $3d$ Rydberg states, and minor for those of the $3p_0$ Rydberg and valence excited states.

To conclude, the present work significantly extends the available DCSs over a comprehensive range of E_0 and θ and provides a more complete picture of their behavior. In this sense, the presently reported electronic excitation DCSs and ICSs contribute to the recently stressed[40] need for individual cross sections for such a prototypical molecule as benzene.

ACKNOWLEDGMENTS

A.G.F. acknowledges support from Coordenação de Aperfeiçoamento de Pessoal de Nível Superior - Brasil (CAPES) - Finance Code 001, and M.A.P.L. and R.F.C. acknowledge the Brazilian agency Conselho Nacional de Desenvolvimento Científico e Tecnológico (CNPq). This research used the computing resources and assistance of the John David Rogers Computing Center (CCJDR) in the Institute of Physics "Gleb Wataghin", University of Campinas. The work at California State University Fullerton (CSUF) was funded by the US National Science Foundation, Research in an Undergraduate Institution, under Grants NSF-RUI AMO 1606905 and 1911702. The Troy High School student M.M. participated in the Troy Tech Summer Internship program. M.A.K. acknowledges the past invaluable help of CSUF technicians J. Woodland, A. Daveler, S. Bhari and R. Wright for building and maintenance of the laboratory.

AUTHOR DECLARATIONS

Conflict of interest

The authors have no conflicts to disclose.

Author Contributions

Alan G. Falkowski: Formal Analysis (equal); Investigation (equal); Visualization (equal); Writing – original draft (equal). **Romarly F. da Costa:** Conceptualization (equal); Supervision (equal); Writing – review and editing (equal). **Marco A. P. Lima:** Conceptualization (equal); Supervision (equal); Writing – review and editing (equal). **Alexi de A. Cadena:** Formal Analysis (equal); Investigation (equal). **Ronald Pocoroba:** Formal Analysis (equal); Investigation (equal). **Regan Jones:** Formal Analysis (supporting); Investigation (supporting). **Mahak Mathur:** Investigation (supporting). **J. G. Childers:** Formal Analysis (equal); Writing – original draft (supporting). **Murtadha A. Khakoo:** Conceptualization (equal); Funding acquisition (equal); Supervision (equal); Writing – review and editing (equal). **Fábris Kossoski:** Conceptualization (equal); Formal Analysis (equal); Supervision (equal); Visualization (equal); Writing – original draft (equal); Writing – review and editing (equal).

DATA AVAILABILITY STATEMENT

The data that support the findings of this study are available from the corresponding author upon reasonable request.

[1] C. Murray, "Bewildering benzene," Nat. Chem. **14**, 584–584 (2022).
[2] B. M. Jones, F. Zhang, R. I. Kaiser, A. Jamal, A. M. Mebel, M. A. Cordiner, and S. B. Charnley, "Formation of benzene in the interstellar medium," Proc. Natl. Acad. Sci. **108**, 452–457 (2011).

[3]L. Du, Y. Wang, K. Wang, and G. Luo, "Preparation of calcium benzene sulfonate detergents by a microdispersion process," Ind. Eng. Chem. Res. **52**, 10699–10706 (2013).

[4]S. Olivera, H. B. Muralidhara, K. Venkatesh, K. Gopalakrishna, and C. S. Vivek, "Plating on acrylonitrile–butadiene–styrene (abs) plastic: a review," J. Mater. Sci. **51**, 3657–3674 (2016).

[5]D. Loomis, K. Z. Guyton, Y. Grosse, F. El Ghissassi, V. Bouvard, L. Benbrahim-Tallaa, N. Guha, N. Vilahur, H. Mattock, and K. Straif, "Carcinogenicity of benzene," Lancet Oncol. **18**, 1574–1575 (2017).

[6]J. A. Bond and H. M. Bolt, "Review of the toxicology of styrene," CRC Crit. Rev. Toxicol. **19**, 227–249 (1989).

[7]H. E. Runion, "Benzene in gasoline," Am. Ind. Hyg. Assoc. J. **36**, 338–350 (1975).

[8]D. K. Verma and K. d. Tombe, "Benzene in gasoline and crude oil: occupational and environmental implications," Am. Ind. Hyg. Assoc. J. **63**, 225–230 (2002).

[9]K. Shang, J. Ren, Q. Zhang, N. Lu, N. Jiang, and J. Li, "Successive treatment of benzene and derived byproducts by a novel plasma catalysis-adsorption process," J. of Environ. Chem. Eng. **9**, 105767 (2021).

[10]T. B. Brill and K. J. James, "Kinetics and mechanisms of thermal decomposition of nitroaromatic explosives," Chem. Rev. **93**, 2667–2692 (1993).

[11]A. Skerbele and E. N. Lassettre, "Electron-impact spectra," J. Chem. Phys. **42**, 395–401 (1965).

[12]F. Read and G. Whiterod, "Electron impact spectroscopy III. calculated cross sections for inelastic scattering from benzene," Proc. Phys. Soc. **85**, 71 (1965).

[13]J. P. Doering and A. J. Williams III, "Low-energy, large-angle electron-impact spectra: Helium, nitrogen, ethylene, and benzene," J. Chem. Phys. **47**, 4180–4185 (1967).

[14]R. Compton, R. Huebner, P. Reinhardt, and L. Christophorou, "Threshold electron impact excitation of atoms and molecules: Detection of triplet and temporary negative ion states," J. Chem. Phys. **48**, 901–909 (1968).

[15]E. N. Lassettre, A. Skerbele, M. A. Dillon, and K. J. Ross, "High-resolution study of electron-impact spectra at kinetic energies between 33 and 100 eV and scattering angles to 16°," J. Chem. Phys. **48**, 5066–5096 (1968).

[16]J. P. Doering, "Low-energy electron-impact study of the first, second, and third triplet states of benzene," J. Chem. Phys. **51**, 2866–2870 (1969).

[17]J. Doering, "Electronic energy levels of benzene below 7 eV," J. Chem. Phys. **67**, 4065–4070 (1977).

[18]T. Ogawa, M. Tsuji, M. Toyoda, and N. Ishibashi, "Emission spectra of benzene, toluene, and xylenes by controlled electron impact," Bull. Chem. Soc. Jpn. **46**, 2637–2642 (1973).

[19]R. Azria and G. Schulz, "Vibrational and triplet excitation by electron impact in benzene," J. Chem. Phys. **62**, 573–575 (1975).

[20]K. C. Smyth, J. A. Schiavone, and R. S. Freund, "Electron impact excitation of fluorescence in benzene, toluene, and aniline," J. Chem. Phys. **61**, 1782–1788 (1974).

[21]K. C. Smyth, J. A. Schiavone, and R. S. Freund, "Electron impact excitation of metastable states of benzene, toluene, and aniline," J. Chem. Phys. **61**, 1789–1796 (1974).

[22]K. C. Smyth, J. A. Schiavone, and R. S. Freund, "Optical emission spectra produced by electron impact excitation of benzene," J. Chem. Phys. **61**, 4747–4749 (1974).

[23]R. P. Frueholz, W. M. Flicker, O. A. Mosher, and A. Kuppermann, "Electronic spectroscopy of benzene and the fluorobenzenes by variable angle electron impact," J. Chem. Phys. **70**, 3057–3070 (1979).

[24]D. Wilden and J. Comer, "High resolution electron impact studies of electric dipole-forbidden states of benzene," J. Phys. B: At. Mol. Opt. Phys. **13**, 627 (1980).

[25]P. Swiderek, M. Michaud, and L. Sanche, "Vibronic structure in the low-lying singlet–triplet transitions of benzene and toluene," J. Chem. Phys. **105**, 6724–6732 (1996).

[26]D. Prajapati, H. Yadav, P. Vinodkumar, C. Limbachiya, A. Dora, and M. Vinodkumar, "Computation of electron impact scattering studies on benzene," Eur. Phys. J. D **72**, 1–13 (2018).

[27]H. Kato, M. Hoshino, H. Tanaka, P. Limão-Vieira, O. Ingólfsson, L. Campbell, and M. J. Brunger, "A study of electron scattering from benzene: Excitation of the $^1B_{1u}$, $^3E_{2g}$, and $^1E_{1u}$ electronic states," J. Chem. Phys. **134**, 134308 (2011).

[28]A. Hiraya and K. Shobatake, "Direct absorption spectra of jet-cooled benzene in 130–260 nm," J. Chem. Phys. **94**, 7700–7706 (1991).

[29]A. Bolovinos, P. Tsekeris, J. Philis, E. Pantos, and G. Andritsopoulos, "Absolute vacuum ultraviolet absorption spectra of some gaseous azabenzenes," J. Mol. Spectrosc. **103**, 240–256 (1984).

[30]A. Dawes, N. Pascual, S. V. Hoffmann, N. C. Jones, and N. J. Mason, "Vacuum ultraviolet photoabsorption spectroscopy of crystalline and amorphous benzene," Phys. Chem. Chem. Phys. **19**, 27544–27555 (2017).

[31]P. M. Johnson, "The multiphoton ionization spectrum of benzene," J. Chem. Phys. **64**, 4143–4148 (1976).

[32]P. Johnson and G. Korenowski, "The discovery of a 3p rydberg state in benzene by three-photon resonant multiphoton ionization spectroscopy," Chem. Phys. Lett. **97**, 53–56 (1983).

[33]O. Christiansen, H. Koch, A. Halkier, P. Jørgensen, T. Helgaker, and A. Sánchez de Merás, "Large-scale calculations of excitation energies in coupled cluster theory: The singlet excited states of benzene," J. Chem. Phys. **105**, 6921–6939 (1996).

[34]P. Sharma, V. Bernales, D. G. Truhlar, and L. Gagliardi, "Valence $\pi\pi^*$ excitations in benzene studied by multiconfiguration pair-density functional theory," J. Phys. Chem. Lett. **10**, 75–81 (2019).

[35]P.-F. Loos, F. Lipparini, M. Boggio-Pasqua, A. Scemama, and D. Jacquemin, "A mountaineering strategy to excited states: Highly accurate energies and benchmarks for medium sized molecules," J. Chem. Theory Comput. **16**, 1711–1741 (2020).

[36]A. G. Falkowski, R. F. da Costa, F. Kossoski, M. J. Brunger, and M. A. Lima, "Electronic excitation of benzene by low energy electron impact and the role of higher lying rydberg states," Eur. Phys. J. D **75**, 1–14 (2021).

[37]K. Regeta, M. Allan, Z. Mašín, and J. D. Gorfinkiel, "Absolute cross sections for electronic excitation of pyrimidine by electron impact," J. Chem. Phys. **144**, 024302 (2016).

[38]R. F. C. Neves, D. B. Jones, M. C. A. Lopes, K. L. Nixon, G. B. da Silva, H. V. Duque, E. M. de Oliveira, R. F. da Costa, M. T. d. N. Varella, M. H. F. Bettega, M. A. P. Lima, K. Ratnavelu, G. García, and M. J. Brunger, "Differential cross sections for electron impact excitation of the electronic bands of phenol," J. Chem. Phys. **142**, 104305 (2015).

[39]D. B. Jones, R. F. da Costa, F. Kossoski, M. T. d. N. Varella, M. H. F. Bettega, G. García, F. Blanco, R. D. White, M. A. P. Lima, and M. J. Brunger, "Integral elastic, vibrational-excitation, electronic-state excitation, ionization, and total cross sections for electron scattering from para -benzoquinone," J. Chem. Phys. **148**, 204305 (2018).

[40]A. García-Abenza, A. I. Lozano, L. Álvarez, J. C. Oller, J. Rosado, F. Blanco, P. Limão-Vieira, and G. García, "Evaluated electron scattering cross section dataset for gaseous benzene in the energy range 0.1–1000 eV," Phys. Chem. Chem. Phys. **25**, 20510–20518 (2023).

[41]D. J. Haxton, Z. Zhang, C. W. McCurdy, and T. N. Rescigno, "Complex potential surface for the $^2B_1$ metastable state of the water anion," Phys. Rev. A **69**, 062713 (2004).

[42]R. da Costa, J. Ruivo, F. Kossoski, M. d. N. Varella, M. H. F. Bettega, D. Jones, M. Brunger, and M. Lima, "An ab initio investigation for elastic and electronically inelastic electron scattering from para-benzoquinone," J. Chem. Phys. **149**, 174308 (2018).

[43]M. Zawadzki, R. Wright, G. Dolmat, M. F. Martin, B. Diaz, L. Hargreaves, D. Coleman, D. V. Fursa, M. C. Zammit, L. H. Scarlett, J. K. Tapley, J. S. Savage, I. Bray, and M. A. Khakoo, "Low-energy electron scattering from molecular hydrogen: Excitation of the $x\,^1\Sigma_g{}^+$ to $b\,^3\Sigma_u{}^+$ transition," Phys. Rev. A **98**, 062704 (2018).

[44]T. Meltzer, J. Tennyson, Z. Mašín, M. C. Zammit, L. H. Scarlett, D. V. Fursa, and I. Bray, "Benchmark calculations of electron impact electronic excitation of the hydrogen molecule," J. Phys. B: At., Mol. Opt. Phys. **53**, 145204 (2020).

[45]P. A. S. Randi, G. M. Moreira, and M. H. F. Bettega, "Electron scattering by formamide: Elastic and electronically inelastic cross sections up to 179 energetically open states," Phys. Rev. A **107**, 012806 (2023).

[46]A. d. A. Cadena, A. G. Falkowski, R. Pocoroba, R. Jones, M. Mathur, J. G. Childers, A. S. Barbosa, M. H. F. Bettega, R. F. da Costa, M. A. P. Lima, F. Kossoski, and M. A. Khakoo, "Cross sections for elastic electron scattering by benzene at low and intermediate energies," Phys. Rev. A **106**, 062825 (2022).

[47]K. Takatsuka and V. McKoy, "Extension of the schwinger variational principle beyond the static-exchange approximation," Phys. Rev. A **24**, 2473

(1981).
[48]K. Takatsuka and V. McKoy, "Theory of electronically inelastic scattering of electrons by molecules," Phys. Rev. A **30**, 1734 (1984).
[49]M. A. Lima, L. M. Brescansin, A. J. da Silva, C. Winstead, and V. McKoy, "Applications of the schwinger multichannel method to electron-molecule collisions," Phys. Rev. A **41**, 327 (1990).
[50]M. H. F. Bettega, L. G. Ferreira, and M. Lima, "Transferability of local-density norm-conserving pseudopotentials to electron-molecule-collision calculations," Phys. Rev. A **47**, 1111 (1993).
[51]M. Zawadzki, M. A. Khakoo, L. Voorneman, L. Ratkovich, Z. Mašín, K. Houfek, A. Dora, R. Laher, and J. Tennyson, "Low energy inelastic electron scattering from carbon monoxide: I. excitation of the $a^3\Pi$, $a'^3\Sigma^+$ and $a^1\Pi$ electronic states," J. Phys. B: At., Mol. Opt. Phys. **53**, 165201 (2020).
[52]M. Zawadzki, M. A. Khakoo, A. Sakaamini, L. Voorneman, L. Ratkovich, Z. Mašín, A. Dora, R. Laher, and J. Tennyson, "Low energy inelastic electron scattering from carbon monoxide: II. excitation of the $b^3\Sigma^+$, $j^3\Sigma^+$, $B^1\Pi^+$, $C^1\Sigma^+$ and $E^1\Pi$ rydberg electronic states," J. Phys. B: At., Mol. Opt. Phys. **55**, 025201 (2022).
[53]ETP Equipe Thermodynamique et Plasmas (ETP) model AF151.
[54]J. N. Brunt, G. C. King, and F. H. Read, "A study of resonance structure in helium using metastable excitation by electron impact with high energy resolution," J. Phys. B: At. Mol. Opt. Phys. **10**, 433 (1977).
[55]ARi Industries Inc., Addison, IL 60101 USA, 1HN040B-16.3 biaxial cable.
[56]C. Beenakker and F. de Heer, "Dissociative excitation of benzene by electron impact," Chem. Phys. Lett. **29**, 89–92 (1974).
[57]A. Yokoyama, X. Zhao, E. J. Hintsa, R. E. Continetti, and Y. T. Lee, "Molecular beam studies of the photodissociation of benzene at 193 and 248 nm," J. Chem. Phys. **92**, 4222–4233 (1990).
[58]T. C. Hsu, J. Shu, Y. Chen, J. J. Lin, Y. T. Lee, and X. Yang, "Dissociation rates of benzene at VUV excitation," J. Chem. Phys. **115**, 9623–9626 (2001).
[59]V. V. Kislov, T. L. Nguyen, A. M. Mebel, S. H. Lin, and S. C. Smith, "Photodissociation of benzene under collision-free conditions: An ab initio/Rice–Ramsperger–Kassel–Marcus study," J. Chem. Phys. **120**, 7008–7017 (2004).
[60]A. Hustrulid, P. Kusch, and J. T. Tate, "The dissociation of benzene (C_6H_6), pyridine (C_6H_5N) and cyclohexane (C_6H_{12}) by electron impact," Phys. Rev. **54**, 1037–1044 (1938).
[61]M. E. Wacks and V. H. Dibeler, "Electron Impact Studies of Aromatic Hydrocarbons. I. Benzene, Naphthalene, Anthracene, and Phenanthrene," J. Chem. Phys. **31**, 1557–1562 (1959).
[62]P. J. Richardson, J. H. D. Eland, and P. Lablanquie, "Charge separation reactions of doubly charged benzene ions," Org. Mass Spectrom. **21**, 289–294 (1986).
[63]H. Kühlewind, A. Kiermeier, and H. J. Neusser, "Multiphoton ionization in a reflectron time-of-flight mass spectrometer: Individual rates of competing dissociation channels in energy-selected benzene cations," J. Chem. Phys. **85**, 4427–4435 (1986).
[64]V. R. Bhardwaj, K. Vijayalakshmi, and D. Mathur, "Dissociative ionization of benzene in intense laser fields of picosecond duration," Phys. Rev. A **59**, 1392–1398 (1999).
[65]H.-P. Fenzlaff and E. Illenberger, "Low energy electron impact on benzene and the fluorobenzenes. formation and dissociation of negative ions," Int. J. Mass Spectrom. **59**, 185–202 (1984).
[66]A. Pysanenko, I. S. Vinklárek, J. Fedor, M. Fárník, S. Bergmeister, V. Kostal, T. Nemirovich, and P. Jungwirth, "Gas phase $C_6H_6^-$ anion: Electronic stabilization by opening of the benzene ring," J. Chem. Phys. **157**, 224306 (2022).
[67]M. Hughes, K. James Jr, J. Childers, and M. Khakoo, "Accurate determination of background scattered electrons in crossed electron–and gas–beam experiments using a movable gas beam source," Meas. Sci. Technol. **14**, 841 (2003).
[68]L. R. Hargreaves, K. M. A, C. Winstead, and V. V McKoy, "Excitation of the lowest electronic transitions in ethanol by low-energy electrons," J. Phys. B: At. Mol. Opt. Phys. **49**, 185201 (2016).
[69]R. F. da Costa, M. T. d. N. Varella, M. H. F. Bettega, and M. A. Lima, "Recent advances in the application of the schwinger multichannel method with pseudopotentials to electron-molecule collisions," Eur. Phys. J. D **69**, 1–24 (2015).
[70]A. G. Falkowski, M. A. Lima, and F. Kossoski, "Electronic excitation of ethanol by low-energy electron impact," J. Chem. Phys. **152**, 244302 (2020).
[71]D. B. Jones, F. Blanco, G. García, R. F. da Costa, F. Kossoski, M. T. d. N. Varella, M. H. F. Bettega, M. A. P. Lima, R. D. White, and M. J. Brunger, "Elastic scattering and vibrational excitation for electron impact on para -benzoquinone," J. Chem. Phys. **147**, 244304 (2017).
[72]D. B. Jones, R. F. da Costa, F. Kossoski, M. T. d. N. Varella, M. H. F. Bettega, F. Ferreira da Silva, P. Limão-Vieira, G. García, M. A. P. Lima, R. D. White, and M. J. Brunger, "Electron-impact electronic-state excitation of para -benzoquinone," J. Chem. Phys. **148**, 124312 (2018).
[73]A. I. Lozano, J. C. Oller, D. B. Jones, R. F. da Costa, M. T. d. N. Varella, M. H. F. Bettega, F. Ferreira da Silva, P. Limão-Vieira, M. A. P. Lima, R. D. White, M. J. Brunger, F. Blanco, A. Muñoz, and G. García, "Total electron scattering cross sections from para-benzoquinone in the energy range 1–200 eV," Phys. Chem. Chem. Phys. **20**, 22368–22378 (2018).
[74]N. Nakashima, M. Sumitani, I. Ohmine, and K. Yoshihara, "Nanosecond laser photolysis of the benzene monomer and eximer," J. Chem. Phys. **72**, 2226–2230 (1980).
[75]N. Nakashima and K. Yoshihara, "Laser photolysis of benzene. V. Formation of hot benzene," J. Chem. Phys. **77**, 6040–6050 (1982).
[76]M. Allan, "Study of triplet states and short-lived negative ions by means of electron impact spectroscopy," J. Electron Spectrosc. Relat. Phenom. **48**, 219–351 (1989).
[77]K. Ralphs, G. Serna, L. R. Hargreaves, M. A. Khakoo, C. Winstead, and V. McKoy, "Excitation of the six lowest electronic transitions in water by 9–20 eV electrons," J. Phys. B: At. Mol. Opt. Phys. **46**, 125201 (2013).
[78]A. Kuppermann, J. K. Rice, and S. Trajmar, "Low-energy, high-angle electron-impact spectrometry," J. Phys. Chem. **72**, 3894–3903 (1968).
[79]D. C. Cartwright, A. Chutjian, S. Trajmar, and W. Williams, "Electron impact excitation of the electronic states of N_2. I. differential cross sections at incident energies from 10 to 50 eV," Phys. Rev. A **16**, 1013–1040 (1977).
[80]T. P. T. Do, K. L. Nixon, M. Fuss, G. García, F. Blanco, and M. J. Brunger, "Electron impact excitation of the $\tilde{a}^3B_{1u}$ electronic state in C_2H_4: An experimentally benchmarked system?" J. Chem. Phys. **136**, 184313 (2012).
[81]M. Inokuti, "Inelastic collisions of fast charged particles with atoms and molecules—the bethe theory revisited," Rev. Mod. Phys. **43**, 297–347 (1971).
[82]F. Gianturco and A. Jain, "The theory of electron scattering from polyatomic molecules," Phys. Rep. **143**, 347–425 (1986).
[83]G. Herzberg and E. Teller, "Schwingungsstruktur der elektronenübergänge bei mehratomigen molekülen," Zeitschrift für Physikalische Chemie **21B**, 410–446 (1933).
[84]T. Azumi and K. Matsuzaki, "What does the term "vibronic coupling" mean?" Photochem. Photobiol. **25**, 315–326 (1977).
[85]E. J. Heller, "The semiclassical way to molecular spectroscopy," Acc. Chem. Res. **14**, 368–375 (1981).
[86]D. J. Tannor and E. J. Heller, "Polyatomic Raman scattering for general harmonic potentials," J. Chem. Phys. **77**, 202–218 (1982).
[87]A. Bernhardsson, N. Forsberg, P.-a. Malmqvist, B. O. Roos, and L. Serrano-Andrés, "A theoretical study of the $^1B_{2u}$ and $^1B_{1u}$ vibronic bands in benzene," J. Chem. Phys. **112**, 2798–2809 (2000).
[88]I. Borges, A. Varandas, A. Rocha, and C. Bielschowsky, "Forbidden transitions in benzene," J. Mol. Struct. THEOCHEM **621**, 99–105 (2003).
[89]G. Herzberg, *Electronic Spectra and Electronic Structure of Polyatomic Molecules*, Molecular spectra and molecular structure (Van Nostrand, 1966).
[90]E. Schow, K. Hazlett, J. G. Childers, C. Medina, G. Vitug, I. Bray, D. V. Fursa, and M. A. Khakoo, Phys. Rev. A **72**, 062717 (2005).
[91]H. Tanaka, M. J. Brunger, L. Campbell, H. Kato, M. Hoshino, and A. R. P. Rau, "Scaled plane-wave born cross sections for atoms and molecules," Rev. Mod. Phys. **88**, 025004 (2016).
[92]M. Allan, R. Čurík, and P. Čársky, "Coupling of electronic and nuclear motion in a negative ion resonance: Experimental and theoretical study of benzene," J. Chem. Phys. **151**, 064119 (2019).
[93]G. Varsányi, *Vibrational Spectra of Benzene Derivatives* (Academic Press, Hungary, 1969).
[94]R. F. C. Neves, D. B. Jones, M. C. A. Lopes, K. L. Nixon, E. M. de Oliveira, R. F. da Costa, M. T. d. N. Varella, M. H. F. Bettega, M. A. P. Lima, G. B. da Silva, and M. J. Brunger, "Intermediate energy electron impact excita-

tion of composite vibrational modes in phenol," J. Chem. Phys. **142**, 194302 (2015).

[95]D. B. Jones, L. Ellis-Gibbings, G. García, K. L. Nixon, M. C. A. Lopes, and M. J. Brunger, "Intermediate energy cross sections for electron-impact vibrational-excitation of pyrimidine," J. Chem. Phys. **143**, 094304 (2015).